



Enhancement of Heat Transfer in a Liquid Metal Flow past a Thermally Conducting and Oscillating Infinite Flat Plate

P. Puvaneswari and K. Shailendhra[†]

*Department of Mathematics, Amrita School of Engineering, Coimbatore, Amrita Vishwa Vidyapeetham,
 Amrita University, India.*

[†] Corresponding Author Email: k_shailendhra@cb.amrita.edu

(Received November 25, 2014; accepted January 30, 2015)

ABSTRACT

The effect of conjugation on the enhancement of heat transfer in a liquid metal flow past a thermally conducting and sinusoidally oscillating infinite flat plate, when a constant temperature gradient is superimposed on the fluid, is investigated. The plate is made up of the materials compatible with the liquid metals used and is considered to be of finite thickness. Analytical solutions for the velocity and the temperature of the fluid and the solid are obtained. The effects of thermal conductivity and the thickness of the plate on the total time averaged heat flux transported and the thermal boundary layer thickness are investigated in detail. It is found that the effects of wall thickness and wall thermal conductivity on the heat flux transported depend on their effects on the transverse temperature gradient at any frequency. The optimum value of wall thickness at which the net heat flux transported attains the maximum value, for each fluid and for each wall material under consideration, is reported. A maximum increase of 46.14 % in the heat flux transported can be achieved by optimizing the wall thickness. A maximum convective heat flux of $1.87 \times 10^8 \text{ W/m}^2$ is achieved using *Na* with *AISI 316* wall. All the results obtained have been compared with the experimental and analytical results reported in the literature and are found to be in good agreement. It is believed that the new insights gained will be of significant use while designing liquid metal heat transfer systems.

Keywords: Heat transfer enhancement; Conjugate heat transfer; Forced convection; Liquid metals; Laminar oscillatory flow.

NOMENCLATURE

A_o	oscillation amplitude		transported per unit area within the boundary layer due to convection
b	half the wall thickness		
c_f	specific heat capacity of the fluid	q_{cond}	dimensional time averaged heat flux transported per unit area within the boundary layer due to conduction
c_s	specific heat capacity of the plate		
k_f	thermal conductivity of the fluid	t	dimensional time
k_s	thermal conductivity of the plate	T_f	temperature in the fluid
k	thermal conductivity ratio	T_s	temperature in the plate
Q	dimensional total time averaged heat flux transported for a w wide plate	u	dimensional velocity component along x axis
Q_1	non-dimensional total time averaged heat flux transported for a w wide plate	x, y	dimensional cartesian coordinates
Q_{conv}	dimensional time averaged heat flux transported within the boundary layer due to convection	y^*	dimensional thermal boundary layer thickness
Q_{cond}	dimensional time averaged heat flux transported within the boundary layer due to conduction	δ	Stokes viscous boundary layer thickness
q_{conv}	dimensional time averaged heat flux	ϕ	longitudinal thermal flux at $x = 0$
		$\hat{\phi}$	time averaged longitudinal thermal flux at $x = 0$

γ	constant temperature gradient	ν	kinematic viscosity of the fluid
η	non-dimensional transverse coordinate	ρ	density of the fluid
η^*	non-dimensional thermal boundary layer thickness	σ	thermal diffusivity ratio
κ_f	thermal diffusivity of the fluid	τ	non-dimensional time
κ_s	thermal diffusivity of the plate	ω	oscillation frequency

1. INTRODUCTION

The concept of enhancement of heat transfer is demanding the constant attention of many scientists and engineers as modern engineering and technology has to deal with very high temperatures and heat transfer rates. For example, heat flux as high as $3.7 \times 10^9 \text{ W/m}^2$ is encountered during carbon sublimation cooling (Bergles 2003).

Kurzweg designed a novel heat transfer device (Patent No: US 4,590,993, May, 1986) for the enhancement of heat transfer, which is by far superior to standard heat pipes, in which the basic idea is to transfer heat at higher rates, without concomitant net mass transfer, by sinusoidal oscillation of liquid metals, under laminar conditions, when a constant axial temperature gradient is maintained. In the present literature of enhancement of heat transfer (Ozawa and Kawamoto 1991; Zhang *et al.* 2011), this device is referred to as “*dream pipe*”. Heat flux as high as 10^{10} W/m^2 can be achieved using this dream pipe, when the fluid is oscillated at high frequency with large tidal displacements (Kurzweg 1985b). This is several orders of magnitude greater than the heat flux achieved in conventional heat pipes. It has been experimentally and theoretically established (Kaviani 1986; Kurzweg and de Zhao 1997; Kurzweg 1985a; Kurzweg 1985b; Kurzweg 1986; Shailendhra and Devi 2011) that in this novel device, a periodic convective heat transport occurs in the axial direction and a periodic conductive heat transport occurs between the fluid core and the boundary layer region of the oscillating flow which ultimately results in enhancement of heat transfer by several orders of magnitude.

This thermal pumping technique involves no net convective mass transfer and hence plays an important role in situations where heat is to be removed at high rates, without accompanying net mass transfer as in cooling of radioactive liquids or hazardous chemical solutions (Kurzweg 1985b). Applications for this heat transfer process are numerous, ranging from devices in which heat is removed from the core of a nuclear reactor without an accompanying mass transfer to an accelerated cooling device

for removing heat in combustion processes (Kurzweg 1985b). Further, this heat transfer process is driven by external oscillations and hence thermal valves can possibly be designed based on this technique which may find applications in the field of cryogenics (Kurzweg 1986).

Dream pipes are desirable and advantageous compared to the conventional heat pipes owing to their remarkable qualities, viz., the operating temperature can be selected optionally, only a low pressure is needed to operate such pipes, the operation start and stop can be freely carried out, both wick device and the vacuum operation are not necessary and the structure is simple and compact. In the case of conventional heat pipes the temperature difference is sufficient to operate whereas for dream pipes an external device for vibrating the liquid such as an electric motor or a compressor has to be provided (Shailendhra and Devi 2011).

Heat transfer systems using liquid metals as the heat carrier are becoming more common because of the excellent heat transport capabilities of liquid metals. Heat transfer systems with cold or softened metals are replaced by systems with liquid metals. Steam engine and turbines have already given a way to machines using liquid metal as the working fluid. Water cooled atomic reactors are being replaced by reactors using a very high temperature zone cooled by actual streams of alkali metals, viz., sodium and potassium or their eutectic mixtures (Shailendhra and Devi 2011).

Heat transfer using oscillatory flow of liquid metals has tremendous applications in cooling of high power electronics and electrical equipments. In Stirling engines the heat flow through heat pipes is oscillatory and the fluid flow is driven by cyclic variations of pressure (Bouvier and Stouffs 2005). Liquid metal heat pipes are used for transporting thermal energy in many high temperature and high power density space and terrestrial power and energy systems (Genk and Tournier 2011) and in space reactor power systems they help in the redundant removal and transport of the fission

power generated in the reactor to the energy conversion sub-system. Indeed, the previous Soviet *RORSAT* radar satellites were powered by *NaK* cooled reactors. *NaK* was also used in the *U.S.SNAP – 10A* fission reactor. Further, the scientists and engineers of *NASA*'s Exploration Technology Development Program Fission Surface Power Systems Project have been carrying out an active research to perform a non-nuclear laboratory demonstration of fission surface power technology using Stirling or Brayton thermal energy conversion which includes a liquid metal (*NaK*) loop to transport the heat to a power conversion unit for electrical energy production. Further, extensive research is being carried out to measure the effects of oscillating flow and pressure on heat transfer to minimize the thermodynamic loss in Stirling Engines (Tew and Geng 1992). The possibility of using alkali metal heat pipes for cooling space nuclear reactors has been demonstrated by several prototype experiments without any reported failures Genk and Tournier (2011). For further details, on liquid metal heat exchanger designs for fission surface power for Moon and Mars surface missions, one may refer to Rodger W. Dyson and Geng (2009).

On the other hand, for the liquid metal heat pipes with *Na*, *NaK* and *K*, the compatible wall materials are nickel, niobium and stainless steel. In such heat pipes, apart from the physical properties of the fluids, the properties of the wall, like its thermal conductivity and thickness also play a significant role and hence several authors have considered the walls to be thermally conducting (Kaviany 1986; Kurzweg 1985b; Kurzweg and de Zhao 1997). Kurzweg (1985b) analysed the same heat transfer technique in the flow between periodically arranged conductive parallel plate channels. Later, Kurzweg and de Zhao (1997) dealt with this novel heat transfer in a circular pipe with an infinitely thick wall and obtained an approximate solution valid for high frequency cases. Further, Kaviany (1990) investigated this enhanced heat transfer technique by considering thermally conducting circular tubes of finite wall thickness. However, the effect of thermal conductivity of the wall on the heat transfer characteristics of the fluid has not been studied. Inaba *et al.* (2000) have studied the effect of the sectional shapes of pipes on the enhancement of longitudinal heat transfer by fluid pulsation with thermally conducting walls. However, they have not analyzed explicitly the effect of thickness or conductivity of the wall on the thermal flux. Later, Inaba *et al.*

(2004) investigated the enhancement of longitudinal heat transfer by fluid oscillation in thermally conducting circular pipes of arbitrary but finite wall thickness and analysed the effects of wall conductivity and thickness for the case of large amplitude of fluid oscillation.

In all the above studies, a periodic pressure gradient produced by moving pistons or membranes is responsible for generating the oscillations in the fluid. Kurzweg and Chen (1988) have shown that the same enhanced heat transfer can occur along rigid walls bounded by a viscous fluid when such walls execute a periodic motion parallel to the fluid - solid interface, when a constant longitudinal temperature gradient is superimposed on the fluid by examining the problem of thermal pumping in the classical Stokes problem of a sinusoidally oscillating flat plate immersed within a viscous fluid of infinite extent. They have investigated the formation and the role of thermal boundary layer in this novel thermal pumping process. In their concluding remarks, Kurzweg and Chen (1988), have stated that plates of finite thickness with heat storage capability should receive future consideration as they expected significant changes in the results, especially when dealing with low Prandtl number fluids such as liquid metals, owing to the change in the boundary conditions reflecting the effect of conjugation. This motivated us to extend the work of Kurzweg and Chen (1988) by considering the plate to be thermally conducting and study the effects of thermal conductivity of the wall and its thickness on the thermal boundary layer thickness and the heat flux transported. This analysis may throw some light on the design of industrial heat exchangers (Walker 1982) like re-generators in which thermally conducting parallel plates of finite thickness are stacked on top of each other with just sufficient space left between them to accommodate the relatively thin fluid layers within which the heat transport occurs.

It must be noted that the present problem of heat transfer in which the walls are thermally conducting is a conjugate heat transfer problem. The effect or level of conjugation depends on various factors and it is more pronounced in the case of unsteady, laminar flow of low Prandtl number fluids such as liquid metals (Dorfman 2010) and all these conditions are satisfied in the present problem.

Incidentally, Kurzweg (1985b) suggested that it may be of advantage in practical heat transfer devices, based on this dream pipe technique, to

use liquid metals as the working fluid as these fluids have large values of $\rho_f c_f \gamma$ where ρ_f and c_f are the density and specific heat capacity of the fluid respectively and γ is the constant temperature gradient. Further, in these liquid metal heat transfer systems, the only suitable and widely used wall materials are stainless steel of grade *AISI316*, *nickel (Ni)* and *niobium (Nb)* (Kelman *et al.* 1950; Reay and Kew 2006). Accordingly, in the present work, the working fluid is considered to be a liquid metal (potassium (*K*), sodium (*Na*), sodium-potassium alloy *NaK* (%22*Na* – %78*K*)) and the wall is considered to be made up of stainless steel of grade *AISI 316*, *Ni* and *Nb* having various thicknesses, ranging from 1.35mm to 7mm, which are commercially available. For further details on the compatibility of the liquids and the wall materials used in the liquid metal heat transfer systems, the operating conditions and other technical issues one might refer to (Reay and Kew 2006).

To the best of the authors' knowledge, this is the very first realistic, explicit and exhaustive investigation on the effect of wall conductivity and thickness on the thermal boundary layer thickness and the net heat flux transported in the context of enhancement of heat transfer by the oscillation technique proposed by Kurzweg using liquid metals and appropriate compatible wall materials of various thicknesses that are commercially available.

The analytic solutions for the velocity and temperature fields are obtained. The results obtained are compared with the results reported in the literature and possible explanations are provided wherever the results are qualitatively different.

The rest of the paper is organized as follows: Section 2 deals with the mathematical formulation and solution, Section 3 discusses the results obtained and finally Section 4 presents briefly the conclusions arrived at.

2. MATHEMATICAL FORMULATION AND SOLUTION

Consider a thermally conducting infinite flat plate with finite thickness oscillating sinusoidally within an unbounded, viscous, incompressible and thermally conducting fluid of infinite extent. The plate is considered to oscillate, parallel to the fluid-solid interface, with an amplitude A_0 and an angular frequency ω . The fluid flow is assumed to be laminar. The thickness of the plate is assumed to be $2b$. The x -axis is taken along the direction of oscillation

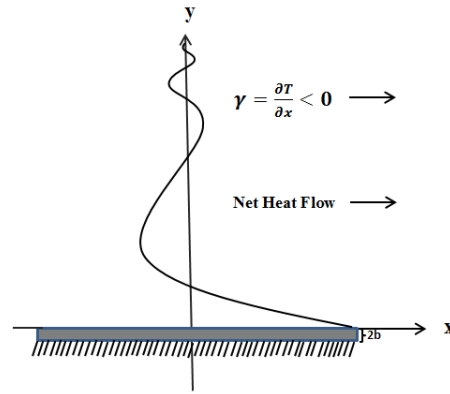


Fig. 1. Schematic representation of the problem.

of the plate and the y -axis is taken vertically upwards. A constant temperature gradient $\gamma = \frac{\partial T_f}{\partial x}$ is superimposed on the fluid in the direction of the oscillation of the plate. Fig1. shows the schematic representation of the problem.

Following the lines of Kurzweg (1986) it is to be noticed that the axial temperature gradient $\frac{\partial T_f}{\partial x}$ is small compared to the very large time dependent transverse temperature gradient $\frac{\partial T_f}{\partial y}$ that exists during most of the sinusoidal cycles which means that $\frac{\partial^2 T_f}{\partial y^2}$ is much larger than $\frac{\partial^2 T_f}{\partial x^2}$ and hence $\frac{\partial T_f}{\partial x}$ is taken as γ which is actually the time averaged value of $\frac{\partial T_f}{\partial x}$. It is pertinent to note that, the maximum value of the thermal boundary thickness is $5.152 \times 10^{-4} \text{ mm}$ (when the fluid is *NaK*). Thus 99% of the heat flux is transported in such a small thickness of fluid layer which is negligibly small compared to the length of the plate. Further the thickness of the plate is also very small (maximum thickness = 7 mm). This fact justifies our assumption that the plate is of infinite length. Owing to this restriction, the present model cannot predict the variation in the thermal boundary layer thickness along the length of the plate in the entrance region.

The governing equations of the problem are

$$\nabla \cdot \vec{q} = 0 \tag{1}$$

$$\rho_f \frac{d\vec{q}}{dt} = \mu \nabla^2 \vec{q} \tag{2}$$

Here, since we consider unidirectional flow along the direction of oscillation of the plate, we assume that the velocity vector is $\vec{q} = (u, 0, 0)$. By eq. (1), it follows that $\frac{\partial u}{\partial x} = 0$ and hence

$u = u(y, t)$. Hence, eq. (2) becomes,

$$\frac{\partial u}{\partial t} = \nu \frac{\partial^2 u}{\partial y^2} \quad (3)$$

where ρ_f is the density, μ is the coefficient of viscosity and $\nu = \frac{\mu}{\rho}$ is the kinematic coefficient of viscosity of the fluid.

The initial and boundary conditions are given by :

$$\begin{aligned} u &= 0 \quad \forall y \geq 0, t \leq 0 \\ u &= A_0 \cos(\omega t), y = 0, t > 0 \\ \text{and } u &= 0, y \rightarrow \infty, t > 0 \end{aligned}$$

We cast the above equations in the non-dimensional form using the following scheme:

$\eta = \frac{y}{\delta}$, $\tau = \omega t$ and $U = \frac{u}{A_0}$ where $\delta = \sqrt{\frac{2\nu}{\omega}}$, the Stokes layer thickness.

Hence, eq. (3) becomes, $\frac{\partial u}{\partial \tau} = \frac{\partial^2 U}{\partial \eta^2}$ and the initial and boundary conditions become

$$\begin{aligned} U &= 0 \quad \forall \eta \geq 0, \tau \leq 0 \\ U &= \cos(\tau), \eta = 0, \tau > 0 \\ \text{and } U &= 0, \eta \rightarrow \infty, \tau > 0 \end{aligned}$$

Assuming $U(\eta, \tau) = \text{Re}[e^{i\tau} f(\eta)]$ (Kurzweg 1985b), it is easy to verify that the dimensional velocity $u(\eta, \tau)$ is given by

$$u(\eta, \tau) = A_0 \omega e^{-\eta} \cos(\tau - \eta), \quad \eta \geq 0, \tau > 0 \quad (4)$$

This is the famous closed form solution of Stoke's oscillating flat plate problem.

The temperatures $T_f(x, y, t)$ and $T_s(x, y, t)$, respectively, in the fluid and in the plate are governed by the corresponding heat equations

$$\rho_f c_f \left[\frac{\partial T_f}{\partial t} + u \frac{\partial T_f}{\partial x} \right] = k_f \left[\frac{\partial^2 T_f}{\partial x^2} + \frac{\partial^2 T_f}{\partial y^2} \right] \quad (5)$$

$$\rho_s c_s \frac{\partial T_s}{\partial t} = k_s \left[\frac{\partial^2 T_s}{\partial y^2} + \frac{\partial^2 T_s}{\partial x^2} \right] \quad (6)$$

where k_f , ρ_f and c_f are the thermal conductivity, the density and the specific heat capacity of the fluid and k_s , ρ_s and c_s are the thermal conductivity, the density and the specific heat capacity of the solid respectively.

Liquid metals are of very low Prandtl numbers and hence viscous dissipation is neglected in equation (5). Infact, the ratios of the viscous dissipation term to the convective term and the diffusion term are $\ll 1$, justifying the neglect of viscous dissipation term.

The appropriate boundary conditions are

$$\begin{aligned} (i) \frac{\partial T_f}{\partial y} &= 0 \text{ as } y \rightarrow \infty \\ (ii) T_f(y) &= T_s(y) \text{ at } y = 0 \\ (iii) k_f \frac{\partial T_f}{\partial y} &= k_s \frac{\partial T_s}{\partial y} \text{ at } y = 0 \\ (or) k \frac{\partial T_f}{\partial y} &= \frac{\partial T_s}{\partial y} \text{ at } y = 0 \text{ where } k = \frac{k_f}{k_s} \\ (iv) k_s \frac{\partial T_s}{\partial y} &= 0 \text{ at } y = -2b \end{aligned}$$

These conditions correspond to the vanishing of heat flux at an infinite distance from the wall, continuity of temperature and heat flux at the fluid solid interface and the heat flux at the insulated bottom of the wall respectively.

Finding exact solutions of the eqns. (5) and (6) subject to the boundary conditions given above is not an easy task. Fortunately, finding such general solutions is not necessary since it is known that the time-averaged value of the axial temperature gradient is constant in this heat transfer process and hence it is enough if one assumes a locally valid temperature distribution of the form

$$T[x, \eta, t] = \gamma [x + \delta g(\eta) e^{i\omega t}]_R$$

which was first proposed by Chatwin (1975).

It should be noted that this form has a physically realistic locally time averaged constant axial temperature gradient and also exhibits a time-dependent cross-stream variation in temperature. Further, Kurzweg (1985b) envisaged that the results obtained, when time-averaged over a period of oscillation, using this approximation and otherwise will not significantly differ provided the Prandtl number Pr and $\omega \Delta x$ are kept sufficiently small. Indeed, Kurzweg (1985a) and Kaviany (1990) have not assumed the above approximation but their time averaged results are not significantly different from the results reported in the literature with the above approximation.

Assuming a temperature distribution, for both the fluid and the solid, in the form proposed by Chatwin (1975) and used by Inaba *et al.* (2004), Kurzweg (1985b), Kurzweg and de Zhao (1997)

and Kaviany (1986), the eqns. (5) and (6) reduce to

$$g_f''(\eta) - 2i Pr g_f(\eta) = Pe \exp(-(1+i)\eta) \quad (7)$$

and

$$g_s''(\eta) - 2i Pr \sigma g_s(\eta) = 0 \quad (8)$$

where $Pr = \nu/\kappa_f$ is the Prandtl number, $Pe = \omega \delta A_0/\kappa_f$ is the Peclet number, $\sigma = \kappa_f/\kappa_s$, $\kappa_f = k_f/(\rho_f c_f)$ and $\kappa_s = k_s/(\rho_s c_s)$ are the thermal diffusivities of the fluid and the solid respectively. Here g_f and g_s represent η -dependent temperature functions within the fluid and the plate respectively.

Solving the equations (7) and (8) subject to the boundary conditions given above, with a little algebraic manipulation, it is easy to see that

$$\begin{aligned} g_f(\eta) &= C_1 \exp(a_1 \eta) + D_1 \exp(-a_1 \eta) + E_1, \\ g_s(\eta) &= C_2 \exp(a_1 \sqrt{\sigma} \eta) + D_2 \exp(-a_1 \sqrt{\sigma} \eta) \end{aligned}$$

where

$$\begin{aligned} a_1 &= \sqrt{2iPr}, \\ a_2 &= A_0 \sqrt{Pr} i/\delta (1 + \sqrt{Pr}), \\ C_1 &= 0, \\ E_1 &= Pe \exp(-(1+i)\eta)/2i(1-Pr), \\ C_2 &= D_2 E_2, \\ E_2 &= \exp(4b\sqrt{2iPr\sigma}/\delta), \\ D_1 &= D_2(1+E_2) + A_0 Pri/(\delta(1-Pr)), \\ D_2 &= a_2 / [(1 + \sqrt{\sigma}/k) E_2 + (1 - \sqrt{\sigma}/k)]. \end{aligned}$$

2.1 Total time averaged heat flux

The net heat flow expressed as longitudinal thermal flux at $x = 0$ is given by

$$\dot{\phi} = \rho_f c_f u T(0, \eta, \tau)$$

On time averaging $\dot{\phi}$ over one period of sinusoidal oscillations, we get

$$\hat{\phi} = E_3 [C_3 + D_3] \sqrt{Pre}^{-a_4 \eta} \quad (9)$$

where

$$\begin{aligned} a_3 &= \sqrt{Pr} - 1, \\ a_4 &= 1 + \sqrt{Pr}, \\ C_3 &= [w_1/a_4] \cos(a_3 \eta), \\ D_3 &= [w_2/a_4 + \sqrt{Pr}/(1-Pr)] \sin(a_3 \eta), \\ E_3 &= \frac{1}{2} \rho_f c_f \gamma A_0^2 \omega, \\ w_1 &= b_1/(b_2 + b_3), \\ b_1 &= 2\sqrt{\sigma}/k \exp(k_1) \sin(k_1), \\ b_2 &= (1 + \sqrt{\sigma}/k)^2 \exp(2k_1) + (1 - \sqrt{\sigma}/k)^2, \\ b_3 &= 2(1 - \sigma/k^2) \exp(k_1) \cos(k_1), \\ w_2 &= (b_4 + b_5)/(b_2 + b_3), \\ b_4 &= (1 + \sqrt{\sigma}/k) \exp(2k_1) \\ b_5 &= 2 \exp(k_1) \cos(k_1) + (1 - \sqrt{\sigma}/k), \\ k_1 &= \exp(4b\sqrt{Pr\sigma}/\delta). \end{aligned}$$

The total time averaged heat transport (Q) for a w wide plate is obtained by integrating (9) over the entire range of η as

$$Q = w\delta \int_0^\infty \hat{\phi} d\eta = -w\delta E_3 Q_1/2 \quad (10)$$

where $Q_1 = H_1 \sqrt{Pr}/(1+Pr)$ is the non-dimensional total time averaged heat transported per unit width of the plate, $H_1 = -w_1 - (w_2 - \sqrt{Pr}/a_3) (a_3/a_4)$.

2.2 Thermal boundary layer thickness

The ratio F of the time averaged flux $\hat{\phi}$ passing through the thickness η of the fluid near the plate of width w to Q is obtained as

$$\begin{aligned} F(\eta) &= w\delta/Q \int_0^\eta \hat{\phi} d\eta \\ &= 1 - H_3 \exp(-a_4 \eta) \end{aligned}$$

where $H_3 = \cos(a_3 \eta) + H_2 \sin(a_3 \eta)$, $H_2 = [w_1 a_3/a_4 - (w_2 - \sqrt{Pr}/a_3)]/H_1$.

The thermal flux boundary layer thickness (η^*) is defined as the value of η for which $F(\eta)$ is 0.99 (Kurzweg and Chen (1988)).

2.3 Enhancement of heat transfer due to oscillation

In order to get a quantitative measure of enhancement of heat transfer in this heat transfer process, it is appropriate to compare the convective heat flux transported (due to oscillation) with the conductive heat flux transported (in the absence of oscillation). Since 99% of the net

convective heat flux is transported within the boundary layer of thickness $y^* = \eta^* \delta$, it is physically practical and mathematically convenient to make the above comparison within the boundary layer, by neglecting 1% of the convective heat flux transported outside the boundary layer.

The total time-averaged heat flux transported by convection within the boundary layer for a wide plate is given by

$$Q_{conv} = w\omega/2\pi \int_0^{2\pi/\omega} \int_0^{y^*} \rho_f c_f u T_f(0, y, t) dy dt.$$

$$= w\delta\sqrt{Pr}E_5 \exp(-a_4\eta^*) + Q$$

where

$$C_4 = [w_1/a_4] \cos(a_3)\eta^*,$$

$$D_4 = \left[w_2/a_4 + \frac{\sqrt{Pr}}{(1-Pr)} \right] \sin(a_3)\eta^*,$$

$$C_5 = [w_1/a_4] \sin(a_3)\eta^*,$$

$$D_5 = \left[w_2/a_4 + \sqrt{Pr}/(1-Pr) \right] \cos(a_3)\eta^*,$$

$$E_4 = a_3(C_5 - D_5) - a_4(C_4 + D_4),$$

$$E_5 = E_3E_4/(2(1+Pr)).$$

Similarly, the total time-averaged heat flux transported by pure conduction across an area of width w and height y^* is given by

$$Q_{cond} = w\omega/2\pi \int_0^{2\pi/\omega} \int_0^{y^*} -k_f \gamma dy dt = -wk_f\gamma y^*.$$

Thus, the time averaged heat fluxes transported per unit area may be computed as

$$q_{conv} = Q_{conv}/(wy^*) \text{ and } q_{cond} = Q_{cond}/(wy^*).$$

3. RESULTS AND DISCUSSION

The purpose of the present investigation is to study the effects of the thermal conductivity and the thickness of the wall on the enhancement of heat transfer in the fluid.

As stated above, K, Na, NaK (%22Na – %78K) are taken as the heat carrying fluid and the wall is considered to be made up of Ni, Nb and stainless steel of grade $AISI316$. The useful operating temperature range ($^{\circ}C$) of heat pipes with K, Na, NaK as the working fluids are 500 – 1000, 600 – 1200 and 425 – 825 respectively (Reay and Kew (2006)). Hence, for the sake of comparing the results, the physical properties of the fluids and the wall materials are considered

at $600^{\circ}C$. Accordingly, the following values are fixed for the various physical quantities (Cengel (2009)).

The thermal conductivities k_f (W / (m K)) and the thermal diffusivities $\kappa_f(m^2/s)$ of K, Na, NaK (%22Na – %78K) are 35.50, 63.63, 28.28 and 6.765×10^{-5} , 6.220×10^{-5} , 4.408×10^{-5} respectively. The Prandtl numbers of these fluids are 0.003143, 0.004202 and 0.00579 respectively. The thermal conductivities k_s (W / (m K)) of the above mentioned wall materials are 65.6, 58.2, 18.3 and the corresponding thermal diffusivities $\kappa_s(m^2/s)$ are 1.39071×10^{-5} , 2.39969×10^{-5} and 4.03893×10^{-6} respectively. We acknowledge the limitation of our modeling in not considering the variation of the physical properties like density, specific heat capacity, kinematic coefficient of viscosity and thermal conductivity with respect to temperature. The thickness of the wall is varied from 1.35 mm to 7 mm which are commercially available. Incidentally, $\epsilon (= b/\delta)$ is defined as the ratio of half the thickness of the wall to the Stokes layer thickness δ . When $\omega = 15$ rad/sec ϵ is varied from 4.00915 to 20.7882 for K , 3.61561 to 18.7476 for Na and 3.65855 to 18.9703 for NaK . The optimum values of ϵ corresponding to the maximum heat flux and the maximum temperature gradient and the optimum boundary layer thickness are obtained and presented in Table. 1 for all the fluids and solids under consideration.

Table 1 Optimum wall thickness for the maximum values of Q_1 and $NTTG$, Optimum Boundary layer thickness and Total heat flux

Fluid	Wall Material			
		Ni	Nb	$AISI 316$
K	ϵ_Q^*	9.6762	13.015	5.2412
	ϵ_T^*	10.517	13.817	5.6292
	η^*	2.4496	2.4512	2.4506
	Q_T ($10^6W/m^2$)	4.0487	3.9358	10.131
Na	ϵ_Q^*	8.5896	10.903	4.4166
	ϵ_T^*	9.4316	10.741	4.5496
	η^*	2.4779	2.4774	2.4779
	Q_T ($10^6W/m^2$)	16.772	16.742	40.856
NaK	ϵ_Q^*	8.6216	11.140	4.6846
	ϵ_T^*	9.5316	10.981	4.8316
	η^*	2.5141	2.5133	2.5150
	Q_T ($10^6W/m^2$)	8.8107	8.7665	21.174

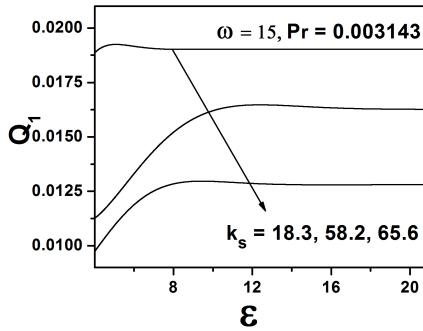


Fig. 2. The effect of wall thermal conductivity on the non-dimensional heat flux transported for K .

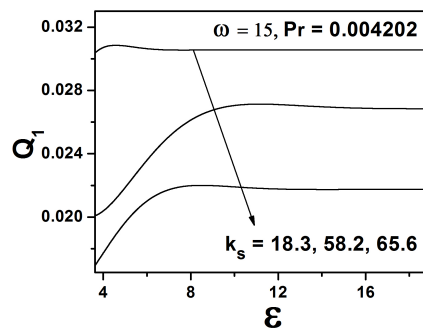


Fig. 3. The effect of wall thermal conductivity on the non-dimensional heat flux transported for Na .

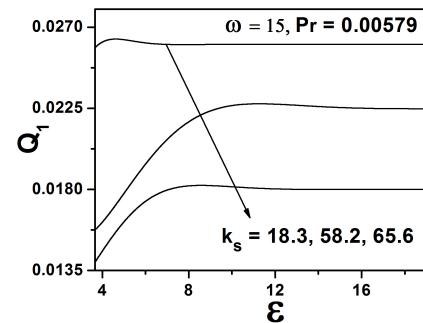


Fig. 4. The effect of wall thermal conductivity on the non-dimensional heat flux transported for NaK .

3.1 The influence of ϵ on the heat flux transported

The physical mechanism for the large axial heat flux achievable in the present heat transfer process is an interchange of heat between the fluid core and the wall. Indeed, the wall contribute to heat transfer by absorbing the thermal energy from the hot fluid and giving off the thermal energy to the cold fluid, during various phases of the oscillation cycle. Hence, the wall thickness

plays a vital role in this heat transfer process.

Figures 2, 3 and 4 depict the variation of Q_1 against ϵ for K , Na , and NaK respectively, for different wall materials. It is observed that when ϵ increases initially Q_1 increases. However, Q_1 attains a constant value for large values of ϵ depending on the material of the wall and the fluid used. The same result was observed by Inaba *et al.* (2004), Kaviany (1986) and Kaviany (1990).

The effect of ϵ on $NTTG$ is presented in Figs. 5, 6 and 7 and using these graphs we render a physical justification for the above observation as follows.

Energy is transferred from more energetic to less energetic molecules when neighboring molecules collide. Conductive heat flow occurs in the direction of the decreasing temperatures since higher temperature are associated with higher molecular energy. By Fourier's law of heat conduction the rate of heat transfer is proportional to the normal temperature gradient. Larger the normal temperature gradient the higher will be the rate of heat transfer. Thus the transverse temperature gradient plays a vi-

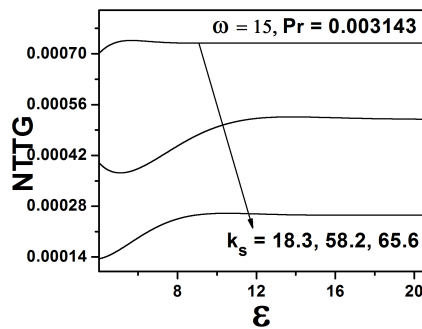


Fig. 5. The effect of wall thermal conductivity on $NTTG$ for K at $\tau = \pi/6$ and $\eta = 0.9$.

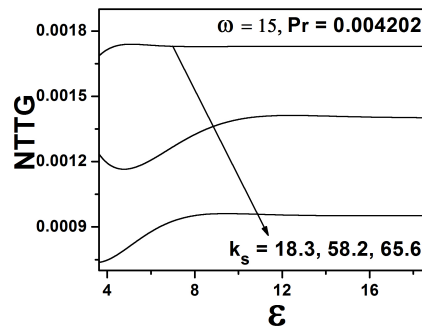


Fig. 6. The effect of wall thermal conductivity on $NTTG$ for Na at $\tau = \pi/6$ and $\eta = 0.9$.

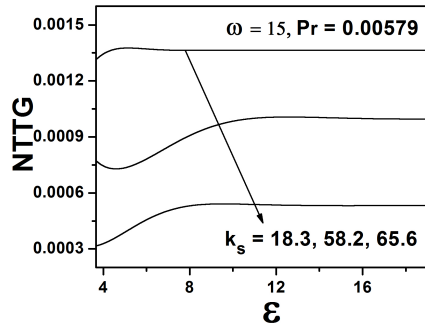


Fig. 7. The effect of wall thermal conductivity on $NTTG$ for NaK at $\tau = \pi/6$ and $\eta = 0.9$.

tal role on the enhancement of heat transfer. Here, it is observed that when ϵ increases the non-dimensional transverse temperature gradient $NTTG$ also increases initially but the effect is saturated beyond a certain wall thickness (Refer Figs. 5, 6 and 7). Moreover, the values of ϵ at which both Q_1 and $NTTG$ attain maximum are approximately the same (Refer Table. 1). Thus, the effect of ϵ on Q_1 depends on the effect of ϵ on $NTTG$. With the fluid K and the wall material Nb , it has been observed that a maximum increase of 46.14 % in the heat flux (Q_1) can be achieved by increasing the wall thickness. It is also observed that ϵ has no effect on Q_1 when the frequency is large. This is because when the frequency is large, the wall thermal penetration distance $d = \sqrt{\frac{2k_s}{\omega}}$ becomes so small and hence the wall thickness doesn't play any role on the enhancement of heat transfer. This result is shown in Figs. 2, 3 and 4 when ϵ is large (ω is large).

3.2 The effect of k_s on the net heat flux transported

In the thermal pumping process considered here, during the forward part of the oscillation, hotter fluid within the core causes a heat flow to the colder portions of the fluid within the boundary layers and to the colder solid walls bounding the fluid. During the other half of the cycle, heat from the hotter fluid in the boundary layers and the walls will diffuse into the fluid core, which is now colder. Therefore the wall thermal conductivity plays an important role in this heat transfer process. Figures 2, 3 and 4 represent the effect of the ratio k of the thermal conductivity of the fluid (k_f) to that of the wall (k_s) on the non-dimensional thermal flux Q_1 . It is observed that when k is increased Q_1 is also increased for each fluid whatever may be the value of ϵ . In other words, when the

thermal conductivity of the wall is increased Q_1 is decreased. In fact, from Table. 2 it is clear that the net heat flux is higher in the case of thermally insulated walls than in the case of thermally conducting walls. This is because a part of the total heat flux transported is conducted through the solid wall when it is thermally conducting and accordingly there is a reduction in the heat flux transported by the fluid when k_s is increased (k is decreased).

It is also observed that $NTTG$ behaves in the same manner as Q in most of the regions of heat transfer which is explained as follows. With Na as the working fluid during the forward part of oscillation, in particular when $\tau = \pi/6$, $NTTG$ decreases as k_s is increased at any wall thickness only beyond $\eta = 0.7$. This result is shown in Fig. 6 when $\eta = 0.9$. The same behavior is observed beyond $\eta = 0.9$ at $\tau = \pi/3$ whatever may be the wall thickness. The effect of k_s on $NTTG$ given above is same for $\tau = \pi/4$ and $\tau = \pi$ only beyond $\eta = 0.8$ and $\eta = 0.5$ respectively whatever may be the value of ϵ . The same result is observed for the other fluid and solid combinations. When the working fluid is K , the same result is observed for $\eta \geq 1.1$, $\eta \geq 0.8$, $\eta \geq 1$ and $\eta \geq 0.6$ at $\tau = \pi/3$, $\tau = \pi/6$, $\tau = \pi/4$ and $\tau = \pi$ respectively whatever may be the wall thickness. Fig. 5 depicts this fact for $\tau = \pi/6$ and $\eta = 0.9$. k_s has the same effect on $NTTG$ for $\eta \geq 1.1$, $\eta \geq 0.8$, $\eta \geq 1$ and $\eta \geq 0.6$ at $\tau = \pi/3$, $\tau = \pi/6$, $\tau = \pi/4$ and $\tau = \pi$ respectively for the fluid NaK irrespective of ϵ . This result is shown in Fig. 7 when $\tau = \pi/6$ and $\eta = 0.9$. Thus, the effect of k_s on Q_1 depends on its effect on $NTTG$ in most of the regions of heat transfer other than the small region closer to the wall.

3.3 The effect of k_s and ϵ on the thermal boundary layer thickness

When the fluid is set into oscillatory axial movement, a time-dependent boundary layer is formed along the plates, and a large transverse temperature gradient is established across the boundary layer. The dependence of the thermal boundary layer thickness (η^*) on the thermal conductivity of the wall (k_s) and ϵ is illustrated in Tables 3, 4 and 5. The results observed are given below.

For a given fluid, the change in thermal boundary layer thickness due to the wall material is

Table 2 Heat flux for thermally conducting and insulated cases

Fluid		Wall Material		
		<i>Ni</i>	<i>Nb</i>	<i>AISI 316</i>
<i>K</i>	Thermally Insulated ($10^4 W/m^2$)	4.7330	4.7330	4.7330
	Thermally Conducting ($10^4 W/m^2$)	1.1595	1.4726	1.7212
<i>Na</i>	Thermally Insulated ($10^5 W/m^2$)	1.32298	1.32298	1.32298
	Thermally Conducting ($10^4 W/m^2$)	4.8023	5.9218	6.7315
<i>NaK</i>	Thermally Insulated ($10^4 W/m^2$)	9.6666	9.6666	9.6666
	Thermally Conducting ($10^4 W/m^2$)	2.5059	3.1287	3.6224

Table 3 Thermal boundary layer thickness η^* for *K* ($Pr = 0.003143$, $\delta = 1.68 \times 10^{-4}$)

$2b(m)$	$\epsilon = \frac{b}{\delta}$	Wall Material		
		<i>Ni</i>	<i>Nb</i>	<i>AISI 316</i>
.00135	4.009	2.628	2.740	2.445
.0015	4.455	2.578	2.700	2.444
.0020	5.939	2.475	2.570	2.460
.0022	6.533	2.456	2.531	2.460
.0023	6.830	2.450	2.514	2.460
.0024	7.127	2.446	2.500	2.460
.0030	8.909	2.445	2.451	2.460
.0040	11.879	2.460	2.446	2.460
.0060	17.819	2.460	2.460	2.460
.0070	20.788	2.460	2.460	2.460

Table 4 Thermal boundary layer thickness η^* for *Na* ($Pr = 0.004202$, $\delta = 1.87 \times 10^{-4}$)

$2b(m)$	$\epsilon = \frac{b}{\delta}$	Wall Material		
		<i>Ni</i>	<i>Nb</i>	<i>AISI 316</i>
.00135	3.616	2.646	2.740	2.476
.0015	4.017	2.600	2.700	2.475
.0020	5.356	2.502	2.585	2.490
.0022	5.892	2.484	2.550	2.490
.0023	6.160	2.479	2.536	2.490
.0024	6.428	2.475	2.523	2.490
.0030	6.696	2.474	2.481	2.490
.0040	8.035	2.490	2.477	2.490
.0060	16.069	2.490	2.490	2.490
.0070	18.748	2.490	2.490	2.490

insignificant as there is only a slight variation in η^* with respect to k_s . η^* becomes a constant as the wall thickness becomes sufficiently

Table 5 Thermal boundary layer thickness η^* for *NaK* ($Pr = 0.00579$, $\delta = 1.84 \times 10^{-4}$)

$2b(m)$	$\epsilon = \frac{b}{\delta}$	Wall Material		
		<i>Ni</i>	<i>Nb</i>	<i>AISI 316</i>
.00135	3.659	2.682	2.800	2.445
.0015	4.065	2.635	2.757	2.444
.0020	5.420	2.539	2.630	2.530
.0022	5.962	2.521	2.592	2.530
.0023	6.233	2.516	2.577	2.530
.0024	6.504	2.512	2.563	2.530
.0030	8.130	2.511	2.517	2.530
.0040	10.840	2.530	2.512	2.530
.0060	16.260	2.530	2.530	2.530
.0070	18.970	2.530	2.530	2.530

large irrespective of the wall material. These constant values of η^* are 2.46 for *K*, 2.49 for *Na* and 2.53 for *NaK*. However, for a given fluid the minimum wall thickness beyond which η^* becomes a constant depends on the wall material. Comparing the Tables 3, 4 and 5, it is observed that when Pr increases η^* also increases whatever the material and the thickness of the wall may be. This result is in good agreement with the results reported in Shailendhra and Devi (1997) for low Prandtl number fluids, in the absence of magnetic field. It is also observed that when ϵ increases η^* decreases up to $\epsilon = 8.90923$, 4.45462 and 11.879 for the fluid *K*, up to $\epsilon = 8.03469$, 4.01734 and 10.7129 for the fluid *Na* and up to $\epsilon = 8.13011$, 4.06506 and 10.8401 for the fluid *NaK* respectively for the wall materials *Ni*, *Nb*, *AISI 316*. These values are very much closer to the values of ϵ up to which $NTTG$ increases for the same fluids and solids (Refer Table. 1 second row). Therefore, for a given temperature difference when the transverse temperature gradient increases η^* decreases. In fact, during most of each cycle, the heat transfer fluid in the boundary layer region adjacent to the wall has a temperature different from that of the core region. Therefore, the temperature difference between the fluid column and the wall is concentrated within the boundary layer. Thinner the boundary layer the greater will be the temperature gradient. Our results are consistent with these facts.

3.4 Convective and conductive heat flux

The values of convective heat flux (q_{conv}) and conductive heat flux (q_{cond}) are found for all the fluids and the solid walls under consideration and are presented in Table. 6. While calculating q_{conv} in each case, the optimum value of the thickness of the wall for which the convective

Table 6. Comparison of convective heat flux per unit area (q_{conv}) with conductive heat flux per unit area (q_{cond}) within the boundary layer

	Fluid	Wall Material		
		Ni	Nb	AISI 316
K	q_{cond} ($10^4 W/m^2$)	0.7704	0.7704	0.7704
	q_{conv} ($10^7 W/m^2$)	3.6035	4.5733	5.3466
	q_{conv}/q_{cond}	4677.7	5936.6	6940.5
Na	q_{cond} ($10^4 W/m^2$)	1.5589	1.5589	1.5589
	q_{conv} ($10^8 W/m^2$)	1.3305	1.6410	1.8650
	q_{conv}/q_{cond}	8534.5	10526	11963
NaK	q_{cond} ($10^4 W/m^2$)	0.7042	0.7042	0.7042
	q_{conv} ($10^7 W/m^2$)	6.9241	8.6477	10.006
	q_{conv}/q_{cond}	9832.9	12281	14209

heat flux is maximum has been considered. It is observed that the time averaged convective heat flux q_{conv} W/m^2 transported is maximum for Na with AISI 316 wall and the maximum value is 1.87×10^8 W/m^2 . In order to analyze the enhancement of heat transfer due to oscillation the ratio q_{conv}/q_{cond} is also computed and presented in Table. 6 for the various fluids and the solid walls considered. In general this ratio varies from 4.678×10^3 to 1.421×10^4 . Thus, due to oscillation heat flux transported is increased by more than an order of 10^3 . The maximum enhancement is observed for NaK with AISI 316.

3.5 Total heat flux transported in the system

The total heat flux transported in the system is calculated as follows.

The total amount of heat transported in the system between $y = -2b$ and $y = y^*$ per unit time (Q_T) is the sum of the amount of heat transported by the fluid in the boundary layer region from $y = 0$ to y^* (in the boundary layer) per unit time (Q_F) and the amount of heat transported by the solid from $y = -2b$ to 0 per unit time (Q_S).

That is

$$Q_T(2b + y^*)W = Q_F + Q_S. \tag{11}$$

By neglecting the axial conduction in the solid, the above equation gives

$$Q_T = \frac{H_1 E_3 \sqrt{Pr} (H_3 e^{-a_4 \eta^*} - 1)}{2(1 + Pr)(2\epsilon + \eta^*)} (W/m^2). \tag{12}$$

The values of Q_T corresponding to the optimum values of η^* and ϵ (Refer Table. 1) are computed for various fluids and solids under consideration and are presented in Table. 1. It is observed that Q_T is maximum for the fluid Na with AISI 316 wall and the maximum heat flux observed is $4.09 \times 10^7 W/m^2$.

3.6 Comparison of our results with earlier results

We would like to compare our results with the earlier works by Kaviany (1990), Kurzweg (1985b), Inaba *et al.* (2004), Kurzweg and de Zhao (1997) and Kurzweg and Chen (1988).

All the results reported in Kurzweg and Chen (1988) can be recovered from the present investigation by taking the limit as $k = k_f/k_s \rightarrow \infty$ or as $b_2 \rightarrow 0$ (insulated plate).

With water as the working fluid and glass as the wall material, Kaviany (1990) found that the effective thermal diffusivity increases as the wall thickness is increased. Similarly Inaba *et al.* (2004) observed that when the pipe inner radius is fixed the heat transfer through the fluid part is more enhanced with increasing thickness of the wall when the working fluid is water and the wall is made of acrylic, glass and copper. They also observed that the effect of wall thickness is saturated beyond a certain wall thickness according to the conductivity of the material. We have also observed that Q_1 increases initially as the wall thickness is increased and it becomes constant for large wall thickness. Therefore, the role of wall thickness on Q_1 depends on whether the wall thickness is small or large. On the other hand, Kurzweg (1985b) reported that the effective thermal diffusivity of the fluid is not affected by the wall thickness when the frequency is large. We have also observed the same result in the case of large frequency. Thus, our results are in good agreement with Inaba *et al.* (2004) and Kurzweg (1985b).

Furthermore, in their parametric analysis, Kurzweg and de Zhao (1997), showed that large quantities of heat can be transported through the tubes when the frequency is large and the thermal conductivity of the wall is higher. But, in the present problem we observed that the heat flux decreases when the thermal conductivity of the wall is increased for each fluid whatever

may be the wall thickness. The discrepancy of the result may be due to the fact that the flow of liquid is confined in a tube in the former case whereas it is unbounded in the present case. Accordingly, the boundary conditions are also different and this discrepancy requires further investigation.

4. CONCLUSIONS

The enhancement of heat transfer in the liquid metal flow past a thermally conducting infinite oscillating flat plate of finite thickness, when a constant temperature is superimposed on the fluid, has been investigated. In general, it is found that both the thickness of the wall and the thermal conductivity of the wall have significant influence on the thermal boundary layer thickness and the total time averaged heat flux, though the effect of thickness of the wall on the boundary layer thickness is not very significant. Following are the results observed:

- For all the fluids under consideration, the total heat flux (Q_1) is enhanced by increasing the ratio (k) of thermal conductivity of the fluid to that of the wall, when the thickness of the wall ($2b$) is fixed.
- As the wall thickness is increased, initially the heat flux Q_1 is also increased. However, when the wall thickness becomes sufficiently large, Q_1 becomes constant depending on the fluid and the wall material used. The optimum value of wall thickness at which Q_1 attains the maximum value, for each fluid and for each wall material under consideration, are tabulated. It is believed that this information will be useful while designing heat transfer systems using this technique.
- The thermal boundary layer thickness (η^*) is not significantly influenced by the wall thickness and it is found that, for a given fluid, as b becomes sufficiently large η^* becomes a constant irrespective of the wall material used.
- The maximum convective heat flux of $1.87 \times 10^8 \text{ W/m}^2$ is achieved using Na with *AISI* 316 wall.
- Due to oscillation, the heat flux transported is increased by more than an order of 10^3 , maximum enhancement of $O(10^4)$ being achieved using NaK with *AISI* 316.
- At $\omega = 15 \text{ rad/sec}$, by choosing a wall of low thermal conductivity, an increase of 46.14 % in the heat flux (Q_1) can be achieved by optimizing the wall thickness.
- When the frequency is very large Q_1 is independent of wall thickness.
- At any frequency, the heat transfer through the fluid is more enhanced with increasing ratio of fluid to wall thermal conductivity, whatever may be the wall thickness.
- The transverse temperature gradient plays an important role on the enhancement of heat transfer.
- The effects of ϵ and k_s on the heat flux transported depend on their effects on *NTTG* at any frequency in most of the regions of heat transfer other than the region very much closer to the wall.
- The total heat flux observed in the system by neglecting the axial conduction in the wall is maximum for the fluid Na with *AISI* 316 wall and the maximum value is $4.09 \times 10^7 \text{ W/m}^2$.

ACKNOWLEDGMENT

We gratefully acknowledge the fruitful discussions we had with Dr. Murali Rangarajan, ASE, Coimbatore.

REFERENCES

- Bergles, A. E. (2003, August). High-flux processes through enhanced heat transfer. In *Keynote 5th Int. Conf. Boiling Heat Transfer*, Montego Bay, Jamaica.
- Bouvier, P. and P. Stouffs (2005). Experimental study of heat transfer in oscillating flow, jean pierre bardon. *Int. J. Heat and Mass Transfer* 48, 2473 – 2482.
- Cengel, Y. A. (2009). *Heat and mass transfer*. New Delhi: Tata McGraw-Hill.
- Chatwin, P. (1975). On the longitudinal dispersion of passive contaminant in oscillating flow in tubes. *J. Fluid Mech.* 71, 513–527.
- Dorfman, A. (2010). *Conjugate problems in convective heat transfer*. New York: CRC Press, Taylor and Francis Group.
- Genk, M. and J.-M. P. Tournier (2011). Uses of liquid metal and water heat pipes in space reactor power systems. *Frontiers in Heat Pipes* 2, 1 – 24.
- Inaba, T., G. Morita, and K. Saitohi (2004). Longitudinal heat transfer enhanced by fluid oscillation in a circular pipe with

- conductive wall. *Heat Trans - Asian Research* 33(2), 129–139.
- Inaba, T., Tahara, and K. Saitoh (2000). Longitudinal heat transfer in oscillatory flows in pipe bundles of various cross sections. *JSME Int. J Ser B* 43, 460–467.
- Kaviany, M. (1986). Some aspects of heat diffusion in fluids by oscillation. *Int. J. Heat and Mass Transfer* 29, 2002–2006.
- Kaviany, M. (1990). Performance of a heat exchanger based on enhanced heat diffusion in fluids by oscillation: Analysis. *Trans ASME J. Heat Transfer* 112, 49–55.
- Kelman, L., W. Wilkinson and L. Yaggee (1950). Resistance of materials to attack by liquid metals.
- Kurzweg, U. (1985a, May). Enhanced heat conduction in flows subjected to sinusoidal oscillations. *ASME J. Heat Transfer* 107, 459–482.
- Kurzweg, U. (1985b, January). Enhanced heat conduction in oscillating viscous flow within parallel-plate channels. *J. Fluid Mechanics* 156, 291–300.
- Kurzweg, U. (1986, April). Temporal and spatial distribution of heat flux in oscillating flow subjected to an axial temperature gradient. *Int. J. Heat and Mass Transfer* 29(12), 1969–1977.
- Kurzweg, U. and J. Chen (1988). Heat transport along an oscillating flat plate. *J. Heat Transfer* 110, 789–790.
- Kurzweg, U. and L. de Zhao (1984). Heat transfer by high-frequency oscillations: A new hydrodynamic technique for achieving large effective thermal conductivities. *Phys.Fluids* 27(11), 2624–2627.
- Ozawa, M. and A. Kawamoto (1991). Lumped parameter modelling of heat transfer enhanced by sinusoidal motion of fluid. *Int. J. Heat and Mass Transfer* 34(12), 3083–3095.
- Reay, D. and P. Kew (2006). *Heat Pipes, fifth ed.* Burlington, USA: Butterworth-Heinemann publications (Elsevier).
- Rodger W. Dyson, Barry Penswick, M. R. and S. M. Geng (2009). Investigation of liquid metal heat exchanger designs for fission surface power.
- Shailendhra, K. and S. A. Devi (1997). Heat transport along on oscillating flat plate in the presence of a transverse magnetic field. *Int. J. Heat and Mass Transfer* 40(2), 498–501.
- Shailendhra, K. and S. A. Devi (2011). On the enhanced heat transfer in the oscillatory flow of liquid metals. *J. Applied Fluid Mechanics* 4(2), 57–62.
- Tew, R. and S. Geng (1992). Overview of nasa supported stirling thermodynamic loss research.
- Walker, G. (1982). *Industrial Heat Exchangers; A Basic Guide.* New York: McGraw-Hill.
- Zhang, X., S. Maruyama and S. Sakai (2011). Numerical investigation of laminar natural convection on a heated vertical plate subjected to a periodic oscillation. *Int. J. Heat and Mass Transfer* 4(2), 4439–4448.